THE JOURNAL OF PHYSICAL CHEMISTRY C

ARTICLE

pubs.acs.org/JPCC

Photoluminescence and Lasing Properties of Catalyst-Free ZnO Nanorod Arrays Fabricated by Pulsed Laser Deposition

Qian Li,[†] Kun Gao,[†,§] Zhigao Hu,[‡] Wenlei Yu,[‡] Ning Xu,[†] Jian Sun,[*,†] and Jiada Wu[*,†]

[†]Key Laboratory of Micro and Nano Photonic Structures, Ministry of Education, Department of Optical Science and Engineering, Fudan University, Shanghai 200433, China

[‡]Key Laboratory of Polar Materials and Devices, Ministry of Education, East China Normal University, Shanghai 200241, China

ABSTRACT: Nearly oriented ZnO nanorods with a mean diameter of ~200 nm and length of 0.8 to 1.7 μm were prepared directly on lattice-mismatched Si (100) substrate by pulsed laser deposition without catalysts. In correlation with the detailed characterization of the morphology, crystalline structure, and oxide phases of the prepared ZnO nanorod arrays, the photoluminescence and lasing properties were studied. At room temperature, the ZnO nanorods emit strong near band edge emission resulting from radiative recombination of free excitons generated by ultraviolet light excitation. The random-lasing-like stimulated emission is observed at high optical pumping at room temperature, which centers around 382.8 nm and results from the superposition of guided lasing modes in different nanorods. The individual peaks as well as the stimulated emission as a whole show red shifts as the pumping intensity increases.

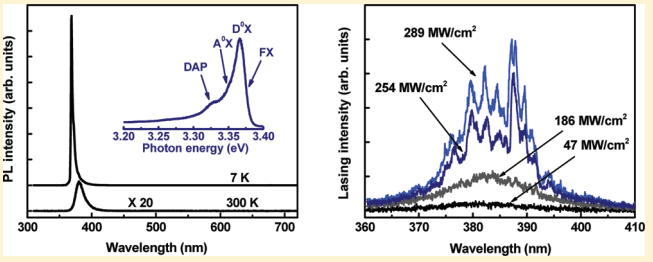

1. INTRODUCTION

Zinc oxide (ZnO) has attracted extensive interests in various fields of fundamental and applied materials research because of its combination of excellent properties such as piezoelectricity, pyroelectricity, conductivity, transparency, thermal, and chemical stability.[1] With a wide direct band gap of 3.37 eV and large exciton binding energy of 60 meV at room temperature, in particular, ZnO is recognized as a promising photonic material in the ultraviolet (UV) region.[2] In addition to the capability of emitting strong luminescence, it has been approved that excitons in ZnO are stable at room temperature, which is believed to contribute to efficient lasing.[3,4] Because of the reports of electron-beam-pumped low-temperature UV lasing from bulk ZnO in 1966,[5] much attention has been attracted to investigate the luminescence and lasing properties of ZnO, either by electrical pumping[6−8] or by optical pumping,[9−12] aiming at short-wavelength light-emitting and lasing devices based on various structured ZnO. In general, fabrication of well-aligned ZnO arrays is an effective approach to realize optoelectronic applications, especially for lasing performance. Lasing activities have been observed in various types of ZnO nanostructures, such as rods, dots, belts, wires, and cones.[3,4,6,10−12] The mechanisms of lasing are regarded as whispering gallery mode lasing[13] and random lasing.[7,8,14] Whispering gallery mode is usually applied for the explanation of lasing from well-faceted ZnO nanostructures, whereas random lasing mode is used for disordered nanostructures.

Various methods have been used to synthesis ZnO nanostructure. Among those methods, pulsed laser deposition (PLD) is suitable to prepare high-purity samples with stoichiometric transfer of the target material to the substrate and convenient to control the structure and composition with versatile deposition parameters. Thin films and various nanostructures of ZnO can also be synthesized by this method. In this article, we report the photoluminescence (PL) and lasing properties of ZnO nanorod arrays grown by PLD from a ZnO target without using any catalysts. At 325 nm light excitation, the ZnO nanorods emit strong UV luminescence, whereas very weak visible luminescence indicates low concentration of defects in the samples. Pumped by a picosecond pulsed laser at room temperature, stimulated light emissions were observed from the ZnO nanorods.

2. EXPERIMENTAL METHODS

2.1. Sample Preparation. ZnO nanorods were synthesized by pulsed laser ablation from a sintered ZnO target with 99.99% in purity. After focusing by a spherical lens, laser pulses (wavelength 532 nm, pulse duration 5 ns, and repetition rate 10 Hz) of the second harmonic of a Q-switched Nd: YAG laser were employed to ablate the ZnO target at an angle of 45° to the surface normal. N-type Si (100) wafers were used as substrates after being chemically cleaned to remove the surface contaminants and natural oxide layer. ZnO nanorods grew directly on lattice-mismatched Si substrate without predepositing any metal catalyzers. The deposition conditions were determined after preliminary trials. The Si substrates were positioned parallel to the target surface with a distance of 40 mm. The deposition chamber was first evacuated

Received: October 28, 2011
Revised: December 17, 2011
Published: December 22, 2011

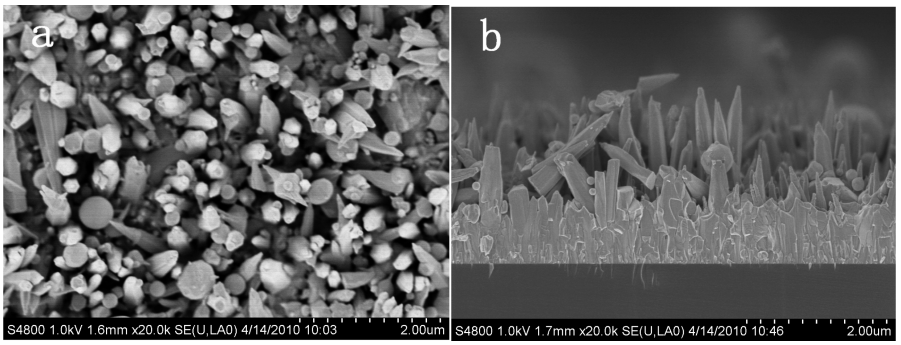

Figure 1. FESEM images of as-deposited ZnO nanorods grown on Si (100) substrate: (a) top view and (b) cross-sectional view.

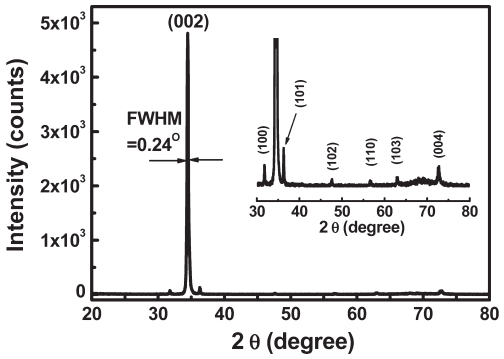

Figure 2. XRD pattern of ZnO nanorods grown on Si (100) substrate. The magnified XRD pattern in the inset shows weak diffractions other than the (002) diffraction.

to a base pressure of 10^{-4} Pa and then filled with 10 Pa oxygen gas, which was used as an oxidizing environment to compensate the loss of oxygen during the transfer of the target material to the film and to stabilize the oxide phase and buffered with argon gas to 2 kPa, which served as the decelerator for the ablated species to avoid impinging damage to the deposited ZnO. The laser fluence on the target surface was set at ~3 J/cm^2. The temperature of the substrate was kept at 600 °C.

2.2. Sample Characterization. The surface morphology of the prepared ZnO nanorods was examined by field-emission scanning electron microscopy (FESEM) with a Hitachi S-4800 microscope. The crystal structure was characterized by X-ray diffraction (XRD) with a Rigaku D/max-γB X-ray diffractometer using a rotating anode operating at 40 kV and 300 mA and Ni-filtered Cu Kα radiation (λ = 0.15406 nm). Fourier-transform infrared (FTIR) spectroscopy and Raman scattering spectroscopy were used for phase identification and structure characterization. FTIR spectroscopy was carried out with a Bruker Vertex 80 V spectrometer. Raman measurements were performed with a Jobin-Yvon LabRAM HR 800 UV micro-Raman spectrometer using 488 nm Ar^+ laser beam and 325 nm He−Cd laser beam to excite the samples.

2.3. Photoluminescence and Lasing Emission Measurements. PL measurements were performed at temperatures from 7 to 300 K for the prepared ZnO nanorods by exciting the samples normally with unpolarized 325-nm laser light from a CW He−Cd laser. The samples were fixed to the cold holder of a closed-cycle cryostat (Arscryo, DE-204) and cooled to the desired temperature. The PL spectra were recorded also at the normal direction by an intensified charge-coupled device (ICCD) (Andor Technology, iStar DH720), which was attached to the exit port of a 0.5 m spectrometer (Acton Research, Spectra Pro 500i). Optical pumping-lasing experiment was performed at room temperature. Under the excitation at normal incidence with 355 nm and 30 ps laser pulses of the frequency-tripled output from a mode-locked Nd:YAG laser working at 10 Hz, the emitted light from the prepared ZnO rods was detected nearly perpendicular to the sample surface. The emission spectra were recorded with an exposure time of 5 s by a charge-coupled device (CCD) (Andor Technology, DV401-BV) in combination with an Acton Spectra Pro 2750 spectrometer.

3. RESULTS AND DISCUSSION

3.1. Sample Morphology. Hexagonal ZnO nanorods with a small size distribution centered at a diameter of ~200 nm and a typical length of 0.8 to 1.7 μm were fabricated on Si substrates. Figure 1 shows the top-view and cross-sectional FESEM images of the as-fabricated ZnO nanorods. As can be clearly seen from the cross-sectional FESEM image, the fabricated ZnO nanorods are nearly oriented, with their axes almost perpendicular to the substrate. At the bottom, the ZnO nanorods grow densely on the substrate surface. They are generally separated from each other at the top with their diameters gradually decreasing from the bottom to the top. Some long rods have sharp tips.

It should be noted that no catalyzers such as metallic Au, Ni were used for the growth of the ZnO nanorods. The ZnO nanorods grew directly on cleaned Si substrate with self-assembled growth process. Hence no such impurities were introduced in the nanorods as well as in the interface between the ZnO rods and the Si substrate. Therefore, ZnO nanorods with high purity were fabricated.

3.2. Crystal Structure. XRD characterization reveals that the prepared ZnO nanorods are of wurzite structure with a preferred orientation along the *c* axis perpendicular to the substrate surface. Figure 2 shows a typical XRD pattern taken from the prepared ZnO nanorods. It can be seen that the (002) diffraction of wurtzite ZnO dominates the XRD pattern, which peaks at 2θ = 34.46° with its full width at half-maximum (fwhm) of 0.24°. In addition, two prominent peaks are identified to be the (101) and (100) diffractions, also indexed to hexagonal wurtzite ZnO, with their intensities much weaker compared with the dominant (002) diffraction. Other orientations are almost indiscernible, as shown in the magnified XRD pattern in the inset of Figure 2. Therefore, the prepared ZnO nanorods are of nanocrystalline nature, and the crystallites are highly oriented with their *c* axes perpendicular to the substrate. From the diffraction angle and the fwhm of the (002) peak, the mean size of the crystallites is calculated to be 35 nm using the Scherrer's formula.[15] The prepared

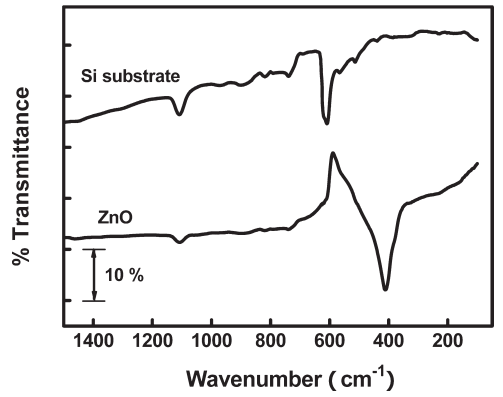

Figure 3. FTIR spectra recorded for prepared ZnO nanorods on Si (100) substrate and for Si substrate.

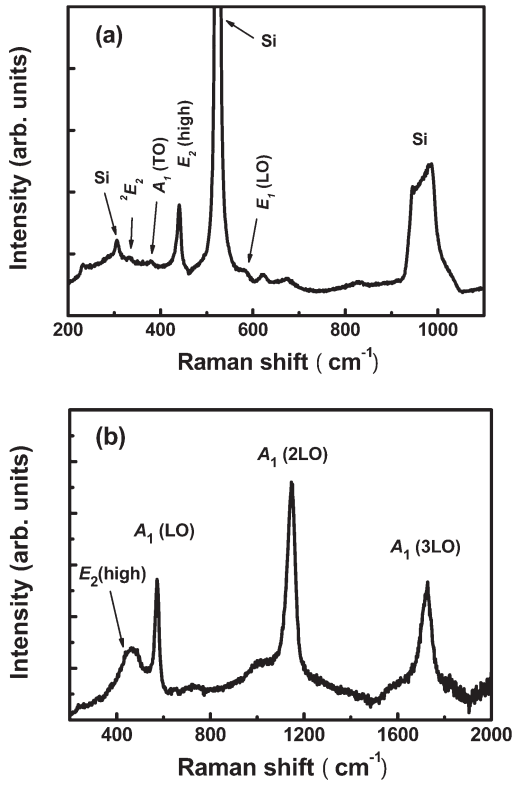

Figure 4. Raman spectra of prepared ZnO nanorods: (a) excited by 488 nm laser and (b) excited by 325 nm laser.

nanorods are therefore not single crystal in structure but are composed of crystallites with average size of 35 nm. Using the well-known X-ray diffraction formula for hexagonal structure,[16] the lattice constants are determined to be a = 0.325 nm and c = 0.520 nm, respectively, from the XRD data. The measured diffraction patterns and the calculated lattice constants are in agreement with the JCPDS data (JCPDS: 36-1451), which suggests that the ZnO rods prepared directly on the cleaned Si (100) substrate are almost stress free.

3.3. Oxide Phase and Vibrational Modes. FTIR measurements were performed in the wavenumber range from 50 to 8000 cm^{-1} for the analysis of the formed oxide phases. Main IR vibrational features are located below 1400 cm^{-1}. The recorded FTIR transmission spectrum in the wavenumber region

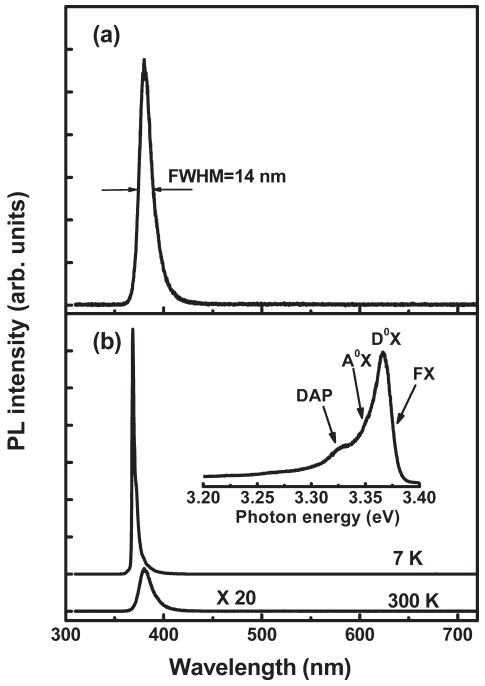

Figure 5. (a) Room temperature PL resulting from 325 nm laser excitation. (b) Comparison of PL spectra recorded at room temperature and at 7 K. The inset in panel b shows the details of the PL recorded at 7 K.

below 1500 cm^{-1} of the prepared ZnO nanorods is displayed in Figure 3 together with that recorded for the Si substrate as a reference. One principal absorption peak is observed around 410 cm^{-1}. This absorption is due to zinc oxide and could be assigned to the stretching mode of Zn−O−Zn, consistent with the frequency that has been theoretically calculated for Zn−O bond excitation in high-quality ZnO.[17]

The results of Raman scattering provide convincing support for the formation of the wurtzite phase in the prepared ZnO nanorods. For hexagonal wurtzite ZnO, the phonon modes belonging to the E_2, E_1, and A_1 symmetries are Raman active.[18] Theoretical calculation has predicted that wurtzite ZnO has six Raman active phonon modes E_2 (low), E_2 (high), A_1 (TO), A_1 (LO), E_1 (TO), and E_1 (LO).[19,20] The Raman spectrum shown in Figure 4a was recorded by exciting the sample with 488 nm laser beam. Besides the signals scattered from the Si (100) substrate, a prominent peak is observed at ∼440 cm^{-1} with its fwhm less than 4 cm^{-1}, which is assigned to the high-frequency branch of ZnO nonpolar optical phonon [E_2 (high)], one of the characteristic modes of wurtzite ZnO.[19,20] A weak but distinct peak is identified near 580 cm^{-1}. This peak is most probably composed of the A_1 LO (574 cm^{-1}) mode and the E_1 LO (583 cm^{-1}) mode.[19,20] In addition, two weak signals can be identified around 332 and 378 cm^{-1}. The former is attributed to the second-order Raman scattering of E_2 mode involving acoustic phonons ($^2E_2$),[21,22] whereas the latter is attributed to the A_1 (TO) mode.[22] The small fwhm of the E_2 (high) peak and the correspondence of the position of the E_2 (high) peak with the phonon of bulk ZnO crystal indicate the good crystal quality of the prepared ZnO rods with strain-free state of the microstructures.

UV light excitation results in a different Raman scattering feature. Figure 4b represents the Raman spectrum of the ZnO nanorods when being excited by 325 nm laser beam with the same backscattering geometry. Besides the scattering band

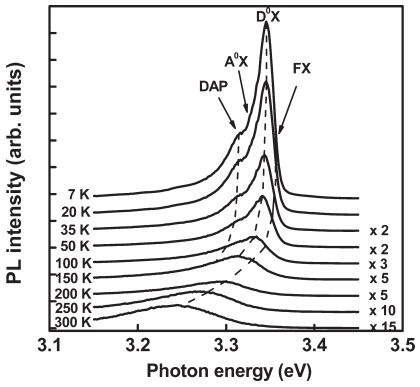

Figure 6. Temperature-dependent PL spectra of ZnO nanorods in the near-band-edge region, showing the evolution of the PL spectra with temperature 7−300 K.

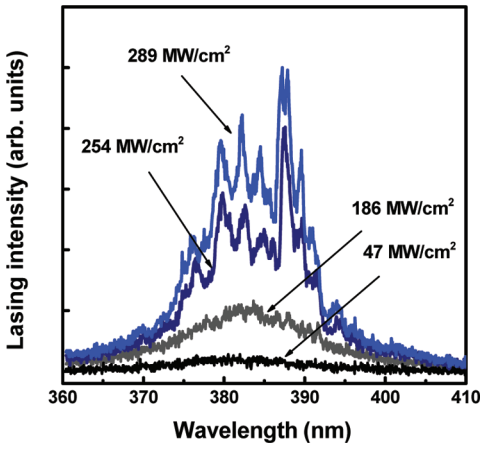

Figure 7. Spontaneous and lasing spectra obtained at different pumping intensities.

centered around 440 cm^{-1} corresponding to the E_2 (high) mode, three prominent peaks at 571, 1150, and 1725 cm^{-1} are observed. They are attributed to the A_1 (LO) mode and its 2- and 3-phonon scattering processes [A_1 (2LO) and A_1 (3LO)]. Intense multiple-phonon scattering processes of the A_1 (LO) modes have previously been observed in UV-resonant Raman scattering from bulk ZnO[23] and ZnO nanoparticles.[24] The above results of Raman scattering measurements provide further evidence in support of good crystal structure of our ZnO nanorods.

3.4. Photoluminescence. At the light excitation with a wavelength of 325 nm at room temperature (300 K), the prepared ZnO nanorods emit strong UV luminescence, as shown in Figure 5a. Green and other visible luminescence bands, which are usually observed from ZnO prepared by various methods can hardly be detected. The UV PL peaks at 382.2 nm (3.244 eV) with an fwhm of 14 nm. This UV luminescence is attributed to the room-temperature free-exciton-related near-band-edge (NBE) emission in ZnO, namely, the recombination of free excitons through an exciton−exciton collision process,[9,25] whereas the visible luminescence is generally believed to be related with different intrinsic deep-level (DL) defects in ZnO such as oxygen vacancy, zinc vacancy, and interstitial zinc.[26,27] The absence of the defect-related visible DL luminescence reveals that the concentrations of such defects are negligible. The strong predominant NBE exciton luminescence together with the absence of DL emission suggests that the prepared ZnO nanorods have good optical properties and can find potential application in UV lasers.

At low temperatures, the NBE luminescence increases significantly with a remarkable blue shift and a much narrower PL width. Figure 5b displays the PL spectrum recorded at 7 K along with that recorded at room temperature for comparison. The NBE luminescence shifts to 368.5 nm (3.365 eV) with an fwhm of 2.5 nm. This luminescence results from the radiative decays from a number of free and bound exciton complexes. The details of PL features related to the emissions with various excitons and their phonon replicas are shown in the inset of Figure 5b. The strongest emission peaking at 3.365 eV is associated with bound excitonic emission at neutral donors (D^0X).[9,28] The NBE luminescence extends to lower energies, and the D^0X peak is accompanied by an emission at 3.345 eV, which can be attributed to the neutral-acceptor bound excitons (A^0X). At the higher energy side of the D^0X peak, the emission associated with free excitons (FX) appears as a shoulder. In addition to the emissions associated with the donor and acceptor bound excitons and that with the free excitons, another PL band is clearly resolved at 3.324 eV. It is most likely from the radiative recombination processes arising from the donor-to-acceptor (DAP) pair transitions.[29]

Figure 6 shows the PL spectra at selected temperatures between 7 and 300 K. It can be seen that as the temperature increases, the luminescence including the A^0X, FX, and DAP components shows obvious red shifts together with significant decrease in intensity. However, the emission associated with bound excitons decreases more rapidly than that associated with free excitons as the temperature increases, and the former is gradually merged into the latter because of the decomposition of bound excitons to free ones with the thermal energy increasing. At the temperature of 200 K, the free exciton emission dominates the NBE luminescence, whereas the bound exciton emission becomes hardly resolvable, indicating that the decomposition of bound excitons to free ones has almost completed. The quenching temperature of this emission is lower than that for bulk ZnO crystals at 210 K[9] but is higher than that reported by Zhong et al. for ZnO nanotips grown on GaN using metalorganic chemical vapor deposition.[30] The transition from the bound exciton emission dominating luminescence to the free exciton dominating one obviously indicates that the dominant room-temperature NBE luminescence results from radiative recombination of free excitons.

3.5. Lasing Emission. The room-temperature lasing characteristics of the ZnO nanorods by optically exciting the sample with a 30 ps pulsed laser pumping are shown in Figure 7. At low pumping intensity, a featureless broad spontaneous emission band ranging from 365 to 400 nm is observed. The intensity of the spontaneous emission increases with the increase in pumping intensity. When the pumping intensity exceeds the threshold, discrete sharp peaks emerge and superpose on the broad emission band. The fwhm of these sharp peaks can be less than 0.6 nm. The emergence of sharp peaks with very narrow line width upon increasing the pumping light intensity suggests the transition from spontaneous emission to stimulated one, that is, the occurrence of the lasing action in the ZnO nanorods. The threshold for lasing was estimated to be ∼180 MW/cm^2. Cao et al. demonstrated that in strongly scattering ZnO polycrystalline films, lasing action could occur in self-formed cavities.[31,32]

It is worthwhile to note that the spacing between the adjacent sharp peaks is not uniform, which resembles a spectrum resulting from a random lasing process. Random lasing phenomenon has been studied in disordered or nanostructured ZnO materials.

In such structures, ZnO provides optical amplification as gain media and light forms close loops by multiple scattering. These loops can serve as laser resonators. For a ZnO nanorod, it can act both as the laser resonator for guided modes and as a gain media for stimulated emission.[33] The lasing emission wavelength is defined by the guided modes of the nanorod. However, our sample is an ensemble of nearly oriented ZnO nanorods with different sizes and lengths. The emission from the sample can be treated as a superposition of guided lasing modes from different nanorods rather than from random lasing due to photon coherent scattering. The emission wavelengths of lasing modes of each nanorod in the ensemble do not coincide exactly with each other. Therefore, the emitted lasing emission on the whole looks much like a random lasing rather than a well-defined one.

The lasing emission is centered around 382.8 nm (3.239 eV), showing a small red shift compared with the peak position of the room-temperature PL, which results from the increase in carrier density and the renormalization of band gap because of high excitation.[34,35] Moreover, it is also observed that the wavelengths of the individual peaks as well as the center of the laser emission depend on the pumping level. These peaks as well as the lasing emission on the whole generally undergo red shifts with the pumping intensity increasing. This can also be attributed to the higher carrier density and the renormalization of band gap, which results in the red shift of the gain at high excitation densities.

4. CONCLUSIONS

We have demonstrated the growth of nearly oriented ZnO nanorods directly on lattice-mismatched Si (100) substrate by pulsed laser deposition without catalysts. The as-grown ZnO nanorods have a mean diameter of ~200 nm and length of 0.8 to 1.7 μm. They are wurzite in crystal structure and almost stress-free with a preferred *c*-axis orientation. At the excitation by 325 nm light at room temperature, the ZnO nanorods emit strong near-band-edge UV luminescence resulting from radiative recombination of free excitons without defect-related visible emission. The near-band-edge PL features both free and bound exciton associated emissions at low temperatures and shows obvious red shifts together with a decrease in luminescence intensity as the measurement temperature increases. The bound exciton-associated emission decreases more rapidly than that associated with free excitons due to the decomposition of bound excitons to free ones as the thermal energy increases. The UV lasing was observed at room temperature by pumping the ZnO nanorods fabricated on Si at pumping intensity above 180 MW/cm^2. The lasing emission resembling a random lasing emission is a superposition of guided lasing modes from different nanorods and shows red shifts as the pumping intensity increases.

AUTHOR INFORMATION

Corresponding Author

*E-mail: jdwu@fudan.edu.cn; jsun@fudan.edu.cn.

Present Addresses

[§]Institute of Ion Beam Physics and Materials Research, Helmholtz-Zentrum Dresden-Rossendorf, Dresden 01314, Germany.

ACKNOWLEDGMENT

We would like to acknowledge the support from the National Basic Research Program of China (contract no. 2012CB934303) and the National Natural Science Foundation of China (contract no. 10875029). Acknowledgment is also made to the Natural Science Foundation of Shanghai (contract no. 10ZR1403900).

REFERENCES

(1) Pearton, S. J.; Norton, D. P.; Ip, K.; Heo, Y. W.; Steiner, T. *Superlattices Microstruct.* **2003**, *34*, 3–32.
(2) Look, D. C.; Claflin, B.; Alivov, Ya I.; Park, S. J. *Phys. Stat. Sol. A* **2004**, *201*, 2203–2212.
(3) Johnson, J. C.; Knutsen, K. P.; Yan, H. Q.; Law, M.; Zhang, Y. F.; Yang, P. D.; Saykally, R. J. *Nano Lett.* **2004**, *4*, 197–204.
(4) Klingshirn, C.; Fallert, J.; Gogolin, O.; Wissinger, M.; Hauschild, R.; Hauser, M.; Kalt, H.; Zhou, H. *J. Lumin.* **2008**, *128*, 792–796.
(5) Nicoll, F. H. *Appl. Phys. Lett.* **1966**, *9*, 13–15.
(6) Hsieh, Y.-P.; Chen, H.-Y.; Lin, M.-Z.; Shiu, S.-C.; Hofmann, M.; Chern, M.-Y.; Jia, X.; Yang, Y.-J.; Chang, H.-J.; Huang, H.-M.; Tseng, S.-C.; Chen, L.-C.; Chen, K.-H.; Lin, C.-F.; Liang, C.-T.; Chen, Y.-F. *Nano Lett.* **2009**, *9*, 1839–1843 .
(7) Zhu, H.; Shan, C.-X.; Zhang, J.-Y.; Zhang, Z.-Z.; Li, B.-H.; Zhao, D.-X.; Yao, B.; Shen, D.-Z.; Fan, X.-W.; Tang, Z.-K.; Hou, X.; Choy, K.-L. *Adv. Mater.* **2010**, *22*, 1877–1881.
(8) Tian, Y.; Ma, X.; Jin, L.; Yang, D. *J. Appl. Phys.* **2010**, *108*, 023517.
(9) Shan, W.; Walukiewicz, W.; Ager, J. W., III; Yu, K. M.; Yuan, H. B.; Xin, H. P.; Cantwell, G.; Song, J. J. *Appl. Phys. Lett.* **2005**, *86*, 191911.
(10) Huang, M. H.; Mao, S.; Feick, H.; Yan, H. Q.; Wu, Y. Y.; Kind, H.; Weber, E.; Russo, R.; Yang, P. D. *Science* **2001**, *292*, 1897–1899.
(11) Dong, H.; Sun, L.; Xie, W.; Zhou, W.; Shen, X.; Chen, Z. *J. Phys. Chem. C* **2010**, *114*, 17369–17373.
(12) Zimmler, M. A.; Capasso, F.; Müller, S.; Ronning, C. *Semicond. Sci. Technol.* **2010**, *25*, 024001.
(13) Gargas, D. J.; Moore, M. C.; Ni, A.; Chang, S. W.; Zhang, Z. Y.; Chuang, S. L.; Yang, P. D. *ACS Nano* **2010**, *4*, 3270–3276.
(14) Kalt, H.; Fallert, J.; Dietz, R. J. B.; Sartor, J.; Schneider, D.; Klingshirn, C. *Phys. Status Solidi B* **2010**, *247*, 1448–1452.
(15) Cullity, B. D.; Stock, S. R. *Elements of X-ray Diffraction*, 3rd ed.; Prentice Hall, Inc: Upper Saddle River, NJ, 2001; p 170.
(16) Cullity, B. D.; Stock, S. R. *Elements of X-ray Diffraction*, 3rd ed.; Prentice Hall, Inc: Upper Saddle River, NJ, 2001; pp 101−103.
(17) Verges, M. A.; Mifsud, A.; Serna, C. J. *J. Chem. Soc., Faraday Trans.* **1990**, *86*, 959–963.
(18) Arguello, C. A.; Rousseau, D. L.; Porto, S. P. S. *Phys. Rev.* **1969**, *181*, 1351–1363.
(19) Damen, T. C.; Porto, S. P. S; Tell, B. *Phys. Rev.* **1966**, *142*, 570–574.
(20) Pachauri, V; Subramaniam, C.; Pradeep, T. *Chem. Phys. Lett.* **2006**, *423*, 240–246.
(21) Rajalakshmi, M.; Arora, A. K.; Bendre, B. S.; Mahamuni, S. *J. Appl. Phys.* **2000**, *87*, 2445–2448.
(22) Cao, B. Q.; Cai, W. P.; Zeng, H. B.; Duan, G. T. *J. Appl. Phys.* **2006**, *99*, 073516.
(23) Scott, J. F. *Phys. Rev. B* **1970**, *2*, 1209–1211.
(24) Wang, Z.; Zhang, H.; Zhang, L.; Yuan, J.; Yan, S.; Wang, C. *Nanotechnology* **2003**, *14*, 11–15.
(25) Ko, J. H.; Chen, Y. F.; Zhu, Z.; Yao, T.; Kobayashi, I.; Uchiki, H. *Appl. Phys. Lett.* **2000**, *76*, 1905–1907.
(26) Vanheusden, K.; Seager, C. H.; Warren, W. L.; Tallant, D. R.; Voigt, J. A. *Appl. Phys. Lett.* **1996**, *68*, 403–405.
(27) Li, D.; Leung, Y. H.; Djurišiæ, A. B.; Liu, Z. T.; Xie, M. H.; Shi, S. L.; Xu, S. J.; Chan, W. K. *Appl. Phys. Lett.* **2004**, *85*, 1601–1603.
(28) Shan, W.; Xie, X. C.; Song, J. J.; Goldenberg, B. *Appl. Phys. Lett.* **1995**, *67*, 2512–2514.
(29) Zhang, B. P.; Binh, N. T.; Segawa, Y.; Wakatsuki, K.; Usami, N. *Appl. Phys. Lett.* **2003**, *83*, 1635–1637.
(30) Zhong, J.; Saraf, G.; Chen, H.; Lu, Y.; Ng, H. M.; SIegrist, T.; Parekh, A.; Lee, D.; Armour, E. A. *J. Electron. Mater.* **2007**, *36*, 654–658.

(31) Cho, S.; Ma, J.; Kim, Y.; Sun, Y.; Wong, G. K. L; Ketterson, J. B. *Appl. Phys. Lett.* **1999**, *75*, 2761–2763.
(32) Wang, C. S.; Chen, Y. L.; Lin, H. Y.; Chen, Y. T.; Chen, Y. F. *Appl. Phys. Lett.* **2010**, *97*, 191104.
(33) Zhou, H.; Wissinger, M.; Fallert, J.; Hauschild, R.; Stelzl, F.; Klingshirn, C.; Kalt, H. *Appl. Phys. Lett.* **2007**, *91*, 181112.
(34) Klingshirn, C.; Hauschild, R.; Fallert, J.; Kalt, H. *Phys. Rev. B* **2007**, *75*, 115203.
(35) Klingshirn, C. *Semiconductor Optics*, 3rd ed.; Springer: Berlin, 2007.